Proceedings of the 16th International Conference on Soil Mechanics and Geotechnical Engineering

doi:10.3233/978-1-61499-656-9-807

The effect of the rate on the cyclic strains in clays – theoretical and laboratory tests

Effet de la vitesse de déformation cycliques pour les argiles – la théorie et les essais de laboratoire

M. Jastrzebska & M. Lupiezowiec
Silesian University of Technology, Gliwice, Poland

ABSTRACT

In this paper, influence of the rate on cyclic strains in cohesive soils is analysed. The authors' aim is a comparison of two different approaches: theoretical and experimental. A new model which is a viscoplastic generalization of the NAHOS (the model able to describe strong nonlinear behavior of soils in the preconsolidation state) is presented. Simultaneously, triaxial tests on kaolin samples were realized with a local measurement of deformation by means of contact free micro displacements sensors. A satisfactory agreement between the theoretical analysis and the experimental results in the preconsolidation state was reached.

RÉSUMÉ

On a présenté une analyse d'influence de la vitesse de déformation sur le comportement des courbes de déformation cyclique. Un modèle élasto-viscoplastique qui a eté proposé vient du modèle NAHOS capable de bien écrire une forte non-linéarité en petites déformations en état de préconsolidation. En même temps on a effectué des essais triaxiaux sur le kaolin à l'aide des capteurs microdéformations sans contact. On a comparé des courbes : théorique et expérimentale présentant l'influence de la vitesse de déformation sur la résistance à la rupture au cisaillement pour les sols cohérents dans l'etat de préconsolidation. Finalement on a obtenu une compatibilité satisfaisante de ce deux courbes.

1 INTRODUCTION

When describing the cyclic loading of soils a nonlinear constitutive model, which is able to characterize a nonlinear behaviour in the overconsolidated state. Soil response also depends on the rate of the loading. Currently applied numerical methods and efficient integration algorithms allow the use of more complicated models in analysis. Furthermore, obtained results are more compatible with experiment.

The constitutive model presented in this paper is a viscoplastic generalization of the NAHOS (Jastrzebska&Sternik, 2004), which simulates behaviour of cohesive soils. The NAHOS model describes the strong changeability of the shear modulus in a small strain interval (10^{-2} to 10^{-1} %) after each sharp bend of a stress path. The sensitivity to the process rate is assured by extending the bounding surface equations and the hardening rule (Lupiezowiec, 2004). On the basis of the previous assumptions, it is possible to create equations of the model similar to occurring in prototype elasto-plastic model, which make possible the application of the integration schemes using in FEM systems.

At the same time, laboratory triaxial tests of the cyclic loading/unloading processes were carried out. These tests were performed on isotropically consolidated samples of prepared kaolin taken from the Porcelain Factory in Tulowice. The laboratory results were compared with the characteristics obtained from the numerical simulation.

2 DESCRIPTION OF THE MODEL

When creating the model equation it was assumed that the total strain ε decomposes into elastic ε^e and inelastic part ε^{vp}, similarly, the elasticity law – identically as in elasto-plastic models. Then, the boundary surface, which separates normally consolidated states (points on the surface) and overconsolidated states (points inside the surface), was defined:

$$F\left(\sigma', p_c, \dot{p_c}\right) = q'^2 + M^2 p'\left(p' - \left(p_c + A\,\dot{p_c}\right)\right) = 0\,, \tag{1}$$

The above-presented equation of the surface depends on the effective stress state, the hardening parameter p_c and its rate. The applied function of boundary surface was a generalized equation presented in the MCC model. The form of the equation enables modeling of the influence of the process rate (Heeres&de Borst, 2001). The inelastic strain rate it calculated from the flow rule, which assumes the direction of the strains as normal to the boundary surface (the associated flow rule).

$$\dot{\boldsymbol{\varepsilon}}^{vp} = \dot{\Lambda}\frac{\partial F}{\partial \sigma'} \tag{2}$$

where positive multiplier $\dot{\Lambda}$ is consistent parameter.

Another created equation is the hardening law one. It describes the relationship between the hardening parameter and the value of inelastic stain:

$$\dot{p_c} = \frac{1+e}{\lambda-\kappa}\,p_c\left(\dot{\varepsilon_v}^{vp} + \xi\exp\left(-\xi_1\varepsilon_s^{vp}\right)\dot{\varepsilon_s}^{vp}\right) - B\exp\left(\frac{q}{q_0}\right)p_c\,, \tag{3}$$

The above-presented form of equation, thanks to the free element on the right side, allows simulation of creep and relaxation, the phenomena which are characteristic in modeling of the viscoplastic bahaviour of materials. That shape of the equation (3) was proposed by Dragon&Mroz (1979). The assumed hardening law includes the dependence on the volumetric strain (which takes place in MCC model) and also on the shear strain (Wilde, 1977). The values A and B present in eq. (1) and (3) are model parameters introduced by the second author (comp. Lupiezowiec, 2003).

The previously mentioned set of equations, assuming the consistent condition:

$$\left(\frac{\partial F}{\partial \sigma'}\right)^T \dot{\sigma}' + \frac{\partial F}{\partial p_c}\dot{\kappa} + \frac{\partial F}{\partial \dot{p}_c}\ddot{p}_c = 0\,, \tag{4}$$

leads into the constitutive equations:

$$\dot{\sigma}' = \mathrm{D}\left(\dot{\varepsilon} - \dot{\Lambda}\frac{\partial F}{\partial \sigma'}\right), \tag{5a}$$

$$s\ddot{\Lambda} + h\dot{\Lambda} + c = 0\,, \tag{5b}$$

where coefficients from the previous formula are defined as follows:

$$s = -M^4 p' A p_c \frac{(1+e)}{\lambda-\kappa}\left[2p' - \left(p_c + A\dot{p}_c\right)\right] - M^2\frac{1+e}{\lambda-\kappa}p' A p_c \cdot 2q'\xi\exp\left(-\xi_1\varepsilon_s^{vp}\right)$$

$$h = -M^4\left[2p' - \left(p_c + A\dot{p}_c\right)\right]^2 K - 12Gq'^2 - M^4\frac{(1+e)}{\lambda-\kappa}\left[2p' - \left(p_c + A\dot{p}_c\right)\right]p'\left(p_c + A\dot{p}_c\right) +$$
$$- M^2\frac{(1+e)}{\lambda-\kappa}p'\cdot 2q\xi\exp\left(-\xi_1\varepsilon_s^{vp}\right)\left(p_c + A\dot{p}_c + Ap_c\dot{\varepsilon}_s^{vp}\right) +$$
$$- M^4\frac{(1+e)}{\lambda-\kappa}p' A p_c\left(2\dot{p} - \dot{p}_c - A\ddot{p}_c\right) - M^2\frac{(1+e)}{\lambda-\kappa}A\cdot 2q' p_c\xi\exp\left(-\xi_1\varepsilon_s^{vp}\right)\,,$$

$$c = KM^2\left[2p' - \left(p_c + A\dot{p}_c\right)\right]\dot{\varepsilon}_V + 6q'G\dot{\varepsilon}_s - M^2 p' B\left(p_c + A\dot{p}_c\right).$$

The above-presented equations are very complex and therefore a numerical method was used to solve them without introducing the closed form of the σ–ε relationship.

For overconsolidated states it was assumed that the plasticity surface is reduced to a point, called the elastic center *S*. Next, for every loading process the radial projection rule occurs (fig. 1), which governs the behaviour of the current point *P*.

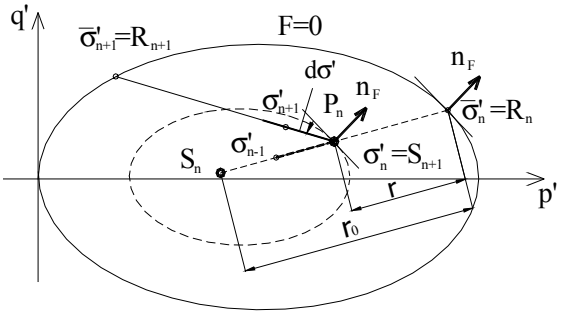

Figure 1. The radial projection rule.

The hardening modulus in point *P* is defined as:

$$K_P = K_R + H\left(\sigma', \varepsilon_v^{vp}, \varepsilon_s^{vp}\right)\cdot\frac{r}{r_0 - r}\,, \tag{6}$$

where: $K_R = \dfrac{\partial F}{\partial p_c}\left(\dfrac{\partial p_c}{\partial \boldsymbol{\varepsilon}^{vp}}\right)^T\left(\dfrac{\partial F}{\partial \sigma'}\right)$ is the hardening modulus in the reflection point *R*, and:

$H = C\left(\dfrac{r}{r_0 - r}\right)^{\mu-1}$ is the hardening function. That form of the function *H* make possible to simulate the strong nonlinearity into small strain interval. Respecting previous assumptions, given in eq. (4b) coefficient *h* takes the below form:

$$h = -M^4\left[2p - \left(p_c + A\dot{p}_c\right)\right]^2 K - 12Gq^2 - M^4\frac{(1+e)}{\lambda-\kappa}\left[2p - \left(p_c + A\dot{p}_c\right)\right]p\left(p_c + A\dot{p}_c\right) +$$
$$- M^2\frac{(1+e)}{\lambda-\kappa}p\cdot 2q\xi\exp\left(-\xi_1\varepsilon_s^{vp}\right)\left(p_c + A\dot{p}_c + Ap_c\dot{\varepsilon}_s^{vp}\right) +$$
$$- M^4\frac{(1+e)}{\lambda-\kappa}pAp_c\left(2\dot{p} - \dot{p}_c - A\ddot{p}_c\right) - M^2\frac{(1+e)}{\lambda-\kappa}A\cdot 2qp_c\xi\exp\left(-\xi_1\varepsilon_s^{vp}\right) + C\left(\frac{r}{r_0 - r}\right)^{\mu}.$$

Unlike in Dafalias&Herrmann proposal (1980), the elastic center *S* is not constant but changes its location after each sharp bend of a stress path (fig. 1). This can be described by the condition:

$$\mathbf{n}^T\cdot d\sigma' < 0\,, \tag{7}$$

where **n** is the unit gradient vector to the boundary surface and $d\sigma'$ – the increase of stress.

When the current point reaches the boundary surface, the further behaviour of the material is governed by formulas derived for the normally consolidated state.

3 LABORATORY TESTING OF SOIL

3.1 *Equipment description*

To perform tests on kaolin samples, conventional triaxial apparatus was used. The triaxial cell contains internal tie bars and a rigid connection between the top cap and the loading piston. The diameters of top cap and pedestal are equal to that of the specimen. Strips of filter paper along specimen and porous stones screwed on top cap and bottom base were used for drainage. The pressure chamber was filled with de-aired water.

Two different measurements of the axial deformation ε_1 were taken:

- Internal ε_1 on the lateral surface of the specimen using two couples of high resolution submergible proximity transducers. The transducers were mounted at two positions, opposite to each other, around the specimen diameter (Fig. 4). Range and resolution of these transducers were 2.0mm and 0.01% respectively.
- External ε_1 using the external displacement gauge fixed on the loading piston.

Lateral deformation ε_s was directly and locally measured by means of a couple of proximity transducers placed in the central part of the specimen. A piece of thin aluminium foil was used as a target. This target was attached to the external membrane with silicone grease (Fig. 4). The data reading took place at chosen time intervals.

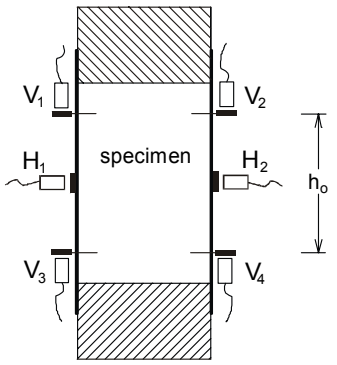

Figure 2. Noncontacting proximity transducers basic configuration.

3.2 *Testing procedure*

The material used in this study came from the Porcelain Factory in Tułowice. Its basic properties are given in Table 1. The tested soil exhibited great homogeneity of structure.

Table 1. Values of some physical properties and classification characteristics of Tulowice kaolin (Jastrzebska 2002).

Specific gravity	G_s	g/cm^3	2.637
Natural water content	w_n	%	33.4-37.7
Liquid limit	w_L	%	42.2
Plastic limit	w_p	%	20.0
Plasticity index	I_p	%	22.2
Liquidity index	I_L	-	0.30-0.35
Skempton's coefficient	A	-	0.52-0.6
Void ratio	e	-	0.956-1.098
Clay fraction	CF	%	37.0-37.9
Silt-size fraction	SF	%	53.7-56.3
Effective cohesion	c'	kPa	10.7
Effective angle of internal friction	ϕ'	°	25
Poisson's ratio	ν	–	0.085

The triaxial tests were carried out on 50mm diameter, 100mm high specimens. Each specimen was fully saturated. At first, they were flushed with de-aired water. Thereafter, a high back pressure was applied. The Bishop's B-values obtained were equal 0.98. Then, the specimens were isotropically consolidated to the value of effective mean pressure p'_c of:
308 kPa in case of undrained test no 12-2,
309 kPa in case of undrained test no 12-3,
307 kPa in case of undrained test no 13-3,
309 kPa in case of undrained test no 13-4.

Next, two of the chosen soil samples were unloaded to effective pressures p'_0 of 109 kPa (test 12-3 and 13-4). These values correspond to the overconsolidation ratios equal to OCR = p'_c/p'_0 = 2.83 for tests 12-3 and 13-4. The tests were provided at various rates: 0.22 mm/h for 12-2 and 12-3 samples and 0.05 mm/h for 13-3 and 13-4 tests.

After isotropic consolidation undrained and drained tests were carried out. Monotonic loading was continued until the value of axial strain $\varepsilon_{unload,1} \approx 1\%$ was reached. Then loading cycles have been applied, 10 cycles in case of undrained tests. In each case, the cycles were performed with constant amplitude of deviatoric stress $q = \sigma_1 - \sigma_3$. Next tests have been continued to 15% of axial strain. Details of tests' conditions are specified in table 2.

Table 2. Test condition of undrained and drained cyclic triaxial compression test on Tulowice kaolin.

Test No	Type of test	OCR	Rate of ε_1 (mm/h)	u_b kPa	σ'_c kPa	B	e_0	$\varepsilon_{unload,1}$ %
12-2	CIU	1.00	0.22	442	308	0.98	1.098	1.58
12-3	CIU	2.83	0.22	441	309	0.98	1.041	1.62
13-3	CIU	1.00	0.05	443	307	0.98	0.986	1.50
13-4	CIU	2.83	0.05	441	309	0.98	0.956	1.38

The graphical results obtained were presented in pictures 2 (tests no. 12-2 and 13-3) and picture 3 (tests 12-3 and 13-4).

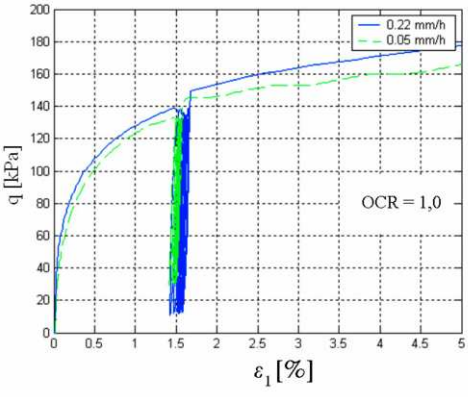

Figure 3. Experimental results of the test in normally consolidated case: q–ε_1 characteristics for test no 12-2 and 13-3 (OCR=1).

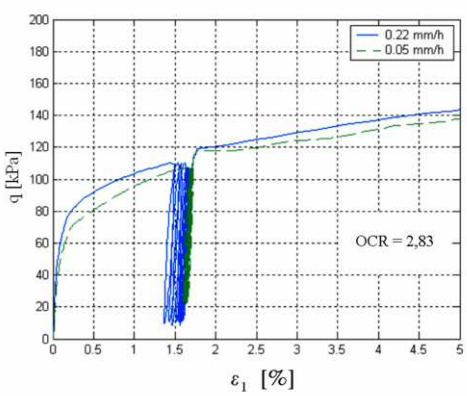

Figure 4. Experimental results of the test in overconsolidated case: q–ε_1 characteristics for tests no 12-3 and 13-4 (OCR=2.83).

4 NUMERICAL SIMULATIONS

The numerical simulations of cyclic compressions in a triaxial apparatus were performed by the Matlab program. This made it possible to calculate complex formulas and to present the obtained results in a simple way. In computation, the implicit predictor–corrector algorithm (Heeres&de Borst, 2001, Lupiezowiec, 2004) was used to solve the constitutive relations (5). In this method, the first step is calculated by means of incremental expressions, and then, the error of the solution **R** is found. It is defined as a vector of differences between values in the current and the previous time step. Then, the derivative of the error vector with respect to the searched quantities was computed and the correction was calculated as:

$$\delta\mathbf{U} = -\left(\frac{\partial\mathbf{R}}{\partial\mathbf{U}}\right)^{-1} \cdot \mathbf{R} \,. \tag{8}$$

where $\delta\mathbf{U}$ is a vector, whose elements, when added to searched quantities, produce a new set of values. That procedure is repeated until the condition:

$$\|\mathbf{R}\| < R_{tol} \tag{9}$$

where R_{tol} is the assumed accuracy of the calculation, is satisfy.

The problem of the behaviour of isotropically consolidated samples was considered. The samples in question (and those unloaded/ additionally uncompressed into the preconsolidation state for the purpose of analysis) were subsequently triaxially undrained loaded to reach $\varepsilon \approx 1{,}5\%$, exposed 10 times to unloading/loading process and finally undrained loading to 15%. Because of isotropic stress and strain state, which occurs in a sample, the numerical analysis concerns only one, isolated point. This assumption simplifies the analysis and it is no longer necessary to solve the whole boundary problem. The initial problem formulation fulfills the laboratory tests conditions described in the previous paragraph.

Numerical simulations were performed with below-presented values of the model parameters:

G = 40.0 MPa,	M = 0.95,	λ = 0.30,	κ = 0.02,
e_0 = 0.75,	ξ = 2.0,	ξ_1 = 1.0,	A = 0.0005 h,
$B = 1 \cdot 10^{-7}$ 1/h,	q_0 = 1,0 kPa.	C = 5 MPa,	μ = 1,0.

The results received from the numerical simulation are presented in pictures 5 and 6, where the q–ε_s characteristics for different velocity of loading process are compared. Figure 5 refers to the normally consolidated case (related to the results shown in fig. 3), while picture 6 - to the overconsolidated state (related to fig. 4).

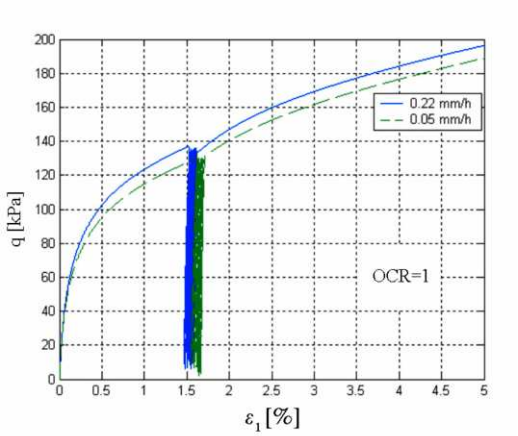

Figure 5. Results of numerical simulations: q–ε_1 characteristics for normally consolidated state (OCR=1).

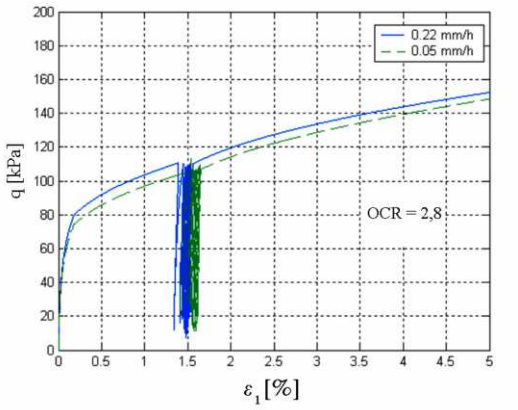

Figure 6. Results of numerical simulations: q–ε_1 characteristics for overconsolidated state (OCR=2.8).

5 CONCLUSIONS

The proposed model shows good qualitative and quantitative agreement with the experimental results. The influence of the rate on the process has been confirmed. The grater the velocity, the greater material response (expressed by shear stress *q*), although the rate does not considerably influence process behaviour in overconsolidated state (fig. 3÷6). It is necessary to emphasize the difference between the value of the strain modulus in the overconsolidated and the normally consolidated state (expressed by the slope of the q–ε_1 characteristic).

The constitutive model presented in the paper is able to simulate the behaviour of material exposed to the complex path of loading. The applied anisotropic hardening rule for the overconsolidated phase makes it possible to simulate the strong changeability of characteristic in a small strain interval. Moreover, the employed boundary equation, which also depends on the rate of the hardening parameter, makes it possible to describe the influence of the loading velocity.

Next step of creation the model should be checking it during analyses of real problem of soil–structure interaction. To do it is needed the implementation of the equations describing model into existing FEM system and performance some example, which ought to be compared with data obtained of monitoring the real investment. That checking could convinced to getting proposed model in practical application.

As the next step in the model creation, it should be verified during analyses of real problems of soil–structure interaction. To do this, the implementation of the equations describing the model in the existing FEM system is needed, followed by performance of some examplary analyses. The results of these ought to be compared with the data obtained from monitoring of the real life investments. Only such verification will confirm the benefits of the model's practical application.

ACKNOWLEDGEMENT

This research was performed within the framework of the project no 5 T07E 038 24 entitled “The nonlinearity of stress-strain characteristics into before-destruction states – experimental bases of the theoretical description”, financed by State Committee for Scientific Research.

REFERENCES

Atkinson J.H. and Bransby P.L., 1978. The mechanics of soils. An introduction to critical state soil mechanics, McGraw-Hill.

Dafalias, Y.F. & Herrmann L.R., 1980. A bounding surface soil plasticity model. In G. N. Pande & O. C. Zienkiewicz (eds), *Soils under Cyclic and Transient Loading; Proc. Int. Symp., Swansea, 7-10 January 1980*: 335-345. Rotterdam:Balkema.

Dragon A. and Mroz Z., 1979. A model for plastic creep of rock-like materials accounting for the kinetics of fracture, Int. J. Rock Mech Sci. & Geomech., Vol. 16, 253-259.

Heeres O. & de Borst R., 2001. A novel rate-dependent subloading model and its implicit integration. *European Conference on Computational Mechanics*, Cracow.

Jastrzebska, M., 2000. Calibrage d’un modèle d’argile à une surface au renforcement anisotrope non lineaire. *XII Colloque Franco-Polonais de Mécanique de Sols et des Roches Appliquée*. Paris, Vol.1.

Jastrzebska, M., 2002. Calibration and verification of a single surface elasto-plasic model for soil with strongly nonlinear anisotropic hardening law. *Ph.D. Thesis (in Polish)*. Silesian Univ. of Technology. Gliwice.

Jastrzebska M., 2004: Identification parametrique et validation d’un modele d’argile preconsolidee elasto-plastique anisotrope non lineaire, *XII Colloque Franco-Polonais de Mécanique de Sols et des Roches Appliquée*, Wrocław, (in press).

Jastrzebska M., Sternik K., 2004. Application of elasto-plastic model with anisotropic hardening to analysis of cyclic loading of cohesive soil, International Conference on „*Cyclic Behaviour of Soils and Liquefaction Phenomena*”, Bochum-Germany.

Lupiezowiec M., 2003. Consistent viscoplastic model – conception and experimental verification, II YGEC, Mamaia–Constanza, 13-14.

Lupiezowiec M., 2004. Consistent single surface elasto-viscoplastic model with strong nonlinear anisotropic hardening for clay soils, *PhD Thesis (in Polish)*, Silesian Univ. of Technology, Gliwice.

Wilde P., 1977. Two invariants dependent model of granular media, Arch. of Mechanics, Vol. 29, 799–809.